Applied Surface Science 268 (2013) 252–258

Contents lists available at SciVerse ScienceDirect

Applied Surface Science

journal homepage: www.elsevier.com/locate/apsusc

Enhancement of visible-light-induced photodegradation over hierarchical porous TiO_2 by nonmetal doping and water-mediated dye sensitization

Lun Pan, Ji-Jun Zou*, Songbo Wang, Zhen-Feng Huang, Xiangwen Zhang, Li Wang

Key Laboratory for Green Chemical Technology of the Ministry of Education, School of Chemical Engineering and Technology, Tianjin University, Tianjin 300072, China

ARTICLE INFO

Article history:
Received 19 October 2012
Received in revised form 2 December 2012
Accepted 11 December 2012
Available online 20 December 2012

Keywords:
Hierarchical TiO_2
Photodegradation
Dye sensitization
Nonmetal doping
Adsorption mode

ABSTRACT

Dye sensitization and nonmetal doping on TiO_2 are important for visible-light utilization in many fields. In this work, N, N&S and N&F doped hierarchical macro-/mesoporous TiO_2 was prepared using hydrothermal method. Most of the nonmetals exist as surface impurities before calcination, without any visible-light response. Thermal calcination makes N effectively implanted into TiO_2 lattice and causes red shift in optical absorption, but S and F are mainly on the surface. The activity of prepared samples for the photodegradation of rhodamine B under visible light was evaluated. The reaction over doped samples without calcination proceeds solely via self-sensitization, and calcination effectively enhances the photodegradation due to nonmetal doping. After being stored for ca. half a year, the activity of all samples are promoted significantly due to the water-mediated adsorption switch from covalent to electrostatic adsorption, caused by pre-bonding of water to surface bridging hydroxyls. The activity of doped samples is further enhanced with water treatment, attributed to the formation of more water-mediated electrostatic modes. The combination of nonmetal doping and water-mediated adsorption switch greatly enhances the visible-light activity of TiO_2 (e.g., water-treated N&F-codoped sample shows 6.8-fold higher activity than pure TiO_2).

© 2012 Elsevier B.V. All rights reserved.

1. Introduction

Visible-light-induced photocatalysis based on TiO_2 has drawn the attention of numerous researchers in the field of water splitting, solar cells, environmental remediation, decomposition of bacteria and so on [1–6]. Great efforts have been made to promote the efficiency of excitation and transfer of photoinduced electrons, and tremendous photosensitizers, including homogeneous sensitizer, heterogeneous catalyst, and dye-sensitized semiconductor have been studied [2–7]. Among these, nonmetal doping and dye sensitization are of the most interest [1–17].

Nonmetal doping of TiO_2 has been conducted for a decade [6]. Asahi et al. made a breakthrough of expanding the visible-light response of TiO_2 by introducing N into the lattice [13]. After that, nonmetal doped semiconductors have been studied intensively, especially for N, S and F doping [9–17]. Generally, the red-shift in the absorption edge is attributed to the impurity state above the valence band (VB) [6], which is vital for the visible-light response and photoactivity of TiO_2.

As to dye sensitization, adsorption on TiO_2 is the prerequisite for electron transfer (ET) from the excited dye to the conduction band of TiO_2 [1,18–25]. There are several adsorption modes: covalent attachment, electrostatic interaction, hydrogen bonding, and so on [25]. Electrostatic interaction was reported to be more effective than the common covalent attachment in photosensitization [1]. Specifically, we recently found that pre-bonding of water molecules on the surface bridging hydroxyls (OH_{br}) of TiO_2 can form $H_3O^+\cdots O_{br}^-$ structure, modulate the adsorption of dye rhodamine B (RhB) from covalent ($Et_2N=R_nCOO—Ti$) to electrostatic ($R_n=N^+Et_2\cdots O_{br}^-$) mode [8]. This water-mediated adsorption switch induces ultrafast ET from RhB to TiO_2 and significantly promotes the self-sensitized photodegradation. This primary work opens a door toward facilely improving the photodegradation of dyes under visible light, in which some factors like surface area and OH_{br} amount would be very important. It also hints that the storage period may show great effect on the performance of photocatalyst because water will be bonded gradually during this period.

Considering the positive effects of nonmetal doping and water-mediated adsorption switch, in this work, we combined the two methods to dramatically enhance the visible-light-induced photoactivity of TiO_2 in the photodegradation of RhB. Hierarchical macro/mesoporous TiO_2 containing bimodal interconnected macroporous and mesoporous structures was chosen, owing to its high surface area, advantages in mass transport and light transmission depth [26–29].

* Corresponding author. Tel.: +86 22 27892340; fax: +86 22 27892340.
E-mail address: jj_zou@tju.edu.cn (J.-J. Zou).

0169-4332/$ – see front matter © 2012 Elsevier B.V. All rights reserved.
http://dx.doi.org/10.1016/j.apsusc.2012.12.074

2. Experimental

2.1. Materials

Tetrabutyl titanate (TBT), urea (CON_2H_4), thiorea (CSN_2H_4), ammonium fluoride (NH_4F), and rhodamine B (RhB) were all reagent grade and purchased from Tianjin Guangfu Fine Chem. Res. Inst. (Tianjin). All reagents were used as received.

2.2. Sample preparation

Doped TiO_2 were synthesized via hydrothermal method. CON_2H_4, CSN_2H_4 and NH_4F were used as the nonmetal sources. The mole ratio of nonmetal to TBT was 1. In a typical synthesis, 10 mL TBT was added dropwise in 150 mL CON_2H_4 (or CSN_2H_4, NH_4F) aqueous solution, subsequently the resulting participate was transferred into a 200 mL Teflon-lined autoclave and heated at 150 °C for 24 h. The obtained powders were filtered, washed with deionized water, and dried at 80 °C overnight. HT refers to the hydrothermal sample without doping while NHT, NFHT and NSHT represent that doped with N, N&F, and N&S, respectively. The samples were then calcined in air at 400 °C for 2 h at a heating rate of 2 °C min^{-1}, namely HT400, NHT400, NFHT400, and NSHT400, respectively.

2.3. Characterization

The crystal parameters of as-prepared samples were determined by a Rigaku D/max 2500v/pc X-ray diffractometer (XRD) equipped with a Cu Kα radiation source. The crystal phase content of TiO_2 and grain size of each phase were calculated according to peak fitting and Scherrer equation ($D = k\lambda/\beta\cos\theta$, where k is a dimensionless constant, 2θ is the diffraction angle, λ is the wavelength of the X-ray radiation, and β is the full width at half-maximum (FWHM) of the diffraction peak), respectively [30,31]. The pore structures were evaluated through N_2 adsorption–desorption isotherms at −196 °C on a Micromeritics TriStar 3000. The surface area and pore distribution were calculated using BET and BJH methods, respectively. SEM images were obtained using a Hitachi S-4800 microscope. UV–vis diffuse reflectance spectra (UV–vis DRS) were recorded with a Hitachi U-3010 spectrometer equipped with a 60 mm diameter integrating sphere using $BaSO_4$ as the reflectance sample. Surface composition, chemical status and total density of state were analyzed by a PHI-1600 X-ray photoelectron spectroscope (XPS) equipped with Al Kα radiation, and the binding energy was calibrated by the C1s peak (284.6 eV) of the contamination carbon. The surface hydroxyl groups were analyzed by the temperature-programmed desorption of ammonia (NH_3-TPD) [32], conducted on a Quantachrome ChemBET TPR/TPD apparatus. The signals of desorbed NH_3 were detected by a thermal conductivity detector (TCD).

2.4. Photocatalytic reaction

Photodegradation of RhB was conducted in a closed quartz chamber (150 mL) vertically irradiated by a 300 W high-pressure xenon lamp (PLS-SXE300UV, Beijing Trusttech. Co. Ltd.). Visible light (>400 nm, 13.0 ± 0.5 mW cm^{-2} at 420 nm) were separated by UV-cut optical filter (Beijing Trusttech. Co. Ltd.). The irradiation area was about 20 cm^2. Reaction conditions: temperature: 20 ± 0.2 °C; C_0(RhB) = 20 μmol L^{-1}; photocatalyst: 0.3 g L^{-1}. After stirring for 30 min in the dark to achieve adsorption equilibrium, the reaction was conducted by magnetic stirring. Samples were withdrawn, centrifuged and analyzed using a Hitachi U-3010 UV-vis spectrometer.

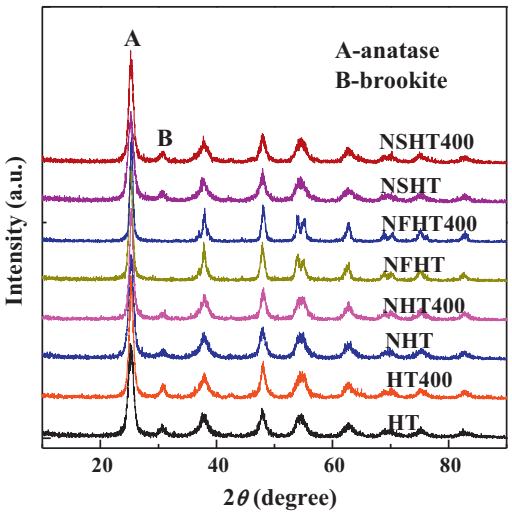

Fig. 1. XRD patterns of as-prepared samples.

3. Results and discussion

3.1. Textual structure

The XRD patterns and N_2 adsorption–desorption isotherms of prepared samples are shown in Figs. 1 and 2, and the structural parameters are summarized in Table 1. HT, NHT and NSHT all show bi-phase of anatase and brookite, whereas N&F codoping inhibits the formation of brookite. In N_2 adsorption isotherms, all the samples exhibit capillary condensation with a large increase in P/P_0 range of 0.2–0.4 and the hysteresis loops are observed for pores with narrow necks and wider bodies (ink-bottle pores, H2 type), indicating the existence of mesopores [6,26,27]. HT, NHT and NSHT have similar S_{BET} (141.7–166.7 m^2 g^{-1}) and average pore size (5.38–6.13 nm), but NFHT shows obviously lower S_{BET} (114.9 m^2 g^{-1}). After calcination at 400 °C, the crystal phase of the samples does not change (except for NSHT400 with the disappearance of brookite phase), but the particle grows up. Even though, HT400, NHT400 and NSHT400 still exhibit similar S_{BET} (94.3–107.4 m^2 g^{-1}) and average pore size (7.38–8.48 nm). But for NFHT400, S_{BET} is significantly decreased to 54.2 m^2 g^{-1} and average pore size is enlarged to 13.46 nm.

Macroporous structure also presents in the samples, as shown in Fig. 3. The introduction of macropores on mesoporous materials is expected to enhance the light transmission depth and diffusion of reactants and products, and thus benefits the photoreaction [26–29]. HT, NHT, NFHT, NSHT and their calcined samples all possess sponge-like porous structure, which is assembled by the randomly distributed intercrossed nanosticks and pores.

Table 1
Textual structures of HMMTs.

Samples	Crystal phase[a]		S_{BET}(m^2 g^{-1})	Average pore size (nm)
	Content (%)	Size (nm)		
HT	(A)86.9/(B)13.1	(A)7.5/(B)7.2	141.7	6.13
HT400	(A)80.5/(B)19.5	(A)9.8/(B)9.0	101.1	8.33
NHT	(A)87.9/(B)12.1	(A)8.4/(B)6.2	154.1	5.97
NHT400	(A)78.7/(B)21.3	(A)15.8/(B)14.0	94.3	8.48
NFHT	(A)100.0	(A)12.4	114.9	5.43
NFHT400	(A)100.0	(A)14.6	54.2	13.46
NSHT	(A)74.6/(B)25.4	(A)7.3/(B)6.8	166.7	5.38
NSHT400	(A)100.0	(A)9.2	107.4	7.38

[a] Abbreviations: A, anatase; B, brookite; R, rutile.

Download English Version:

https://daneshyari.com/en/article/5360654

Download Persian Version:

https://daneshyari.com/article/5360654

Daneshyari.com